

# Phenomenological extraction of two-photon exchange amplitudes from elastic electron-proton scattering cross section data

I. A. Qattan<sup>1</sup>

<sup>1</sup>*Khalifa University of Science and Technology, Department of Physics, P.O. Box 127788, Abu Dhabi, UAE*

(Dated: July 18, 2018)

**Background:** The inconsistency in the results obtained from the Rosenbluth separation method and the high- $Q^2$  recoil polarization results on the ratio  $\mu_p G_E^p/G_M^p$  implies a systematic difference between the two techniques. Several studies suggested that missing higher order radiative corrections to elastic electron-proton scattering cross section  $\sigma_R(\varepsilon, Q^2)$  and in particular hard two-photon-exchange (TPE) effect contributions could account for the discrepancy.

**Purpose:** In this work, I improve on and extend to low- and high- $Q^2$  values the extractions of the  $\varepsilon$  dependence of the real parts of the TPE amplitudes, relative to the magnetic form factor, as well as the ratio  $P_t/P_l^{\text{Born}}(\varepsilon, Q^2)$  using world data on  $\sigma_R(\varepsilon, Q^2)$  with an emphasis on precise new data covering the low-momentum region which is sensitive to the large-scale structure of the nucleon.

**Method:** I combine cross section and polarization measurements of elastic electron-proton scattering to extract the TPE amplitudes. Because the recoil polarization data were confirmed “*experimentally*” to be essentially independent of  $\varepsilon$ , I constrain the ratio  $P_t/P_l(\varepsilon, Q^2)$  to its  $\varepsilon$ -independent term (Born value) by setting the TPE contributions to zero. That allows for the amplitude  $Y_M(\varepsilon, Q^2)$  and  $\sigma_R(\varepsilon, Q^2)$  to be expressed in terms of the remaining two amplitudes  $Y_E(\varepsilon, Q^2)$  and  $Y_3(\varepsilon, Q^2)$  which in turn were parametrized as second-order polynomials in  $\varepsilon$  and  $Q^2$  to reserve as possible the linearity of  $\sigma_R(\varepsilon, Q^2)$  as well as to account for possible nonlinearities in the TPE amplitudes. Further, I impose the Regge limit which ensures the vanishing of the TPE contributions to  $\sigma_R(\varepsilon, Q^2)$  and the TPE amplitudes in the limit  $\varepsilon \rightarrow 1$ .

**Results:** I provide simple parametrizations of the TPE amplitudes, along with an estimate of the fit uncertainties. The extracted TPE amplitudes are compared to previous phenomenological extractions and TPE calculations. The  $P_t/P_l^{\text{Born}}$  ratio is extracted using the new parametrizations of the TPE amplitudes and compared to previous extractions, TPE calculations, and direct measurements at  $Q^2 = 2.50$  (GeV/c)<sup>2</sup>.

**Conclusions:** The extracted TPE amplitudes are on the few-percentage-points level, and behave roughly linearly with increasing  $Q^2$  where they become nonlinear at high  $Q^2$ . On the contrary to  $Y_M$  which is influenced mainly by elastic contributions, I find  $Y_E$  to be influenced by inelastic contributions at large  $Q^2$  values. While  $Y_E$  and  $Y_3$  differ in magnitude, they have opposite sign and tend to partially cancel each other. This suggests that the TPE correction to  $\sigma_R(\varepsilon, Q^2)$  is driven mainly by  $Y_M$  and to a lesser extent by  $Y_3$  in agreement with previous phenomenological extractions and hadronic TPE calculations.

PACS numbers: 25.30.Bf, 13.40.Gp, 14.20.Dh

## I. INTRODUCTION

The electromagnetic form factors of the nucleon  $G_E^{(p,n)}$  and  $G_M^{(p,n)}$ , known as the Sachs form factors [1], are fundamental quantities in nuclear and elementary particle physics since they are used to parameterize the internal structure of the nucleon. Such a parameterization is our way to describe the deviation of the nucleon from the point-like particle picture. Clearly, precise knowledge of these form factors is important since they are an essential ingredient in many calculations and analyses. The Sachs form factors are functions of the four-momentum transfer squared,  $Q^2$ , only. They can be expressed in terms of the Dirac,  $F_1^{(p,n)}(Q^2)$ , and Pauli,  $F_2^{(p,n)}(Q^2)$ , form factors as

$$\begin{aligned} G_E^{(p,n)}(Q^2) &= F_1^{(p,n)}(Q^2) - \tau F_2^{(p,n)}(Q^2), \\ G_M^{(p,n)}(Q^2) &= F_1^{(p,n)}(Q^2) + F_2^{(p,n)}(Q^2), \end{aligned} \quad (1)$$

where  $\tau = Q^2/4M_N^2$ , and  $M_N$  is the mass of the nucleon.

In elastic electron-proton scattering, the reduced cross section  $\sigma_R$ , which is simply the measured differential cross section multiplied by a kinematic factor, can be

expressed in terms of  $G_E^p$  and  $G_M^p$  as

$$\sigma_R = \frac{d\sigma}{d\Omega} \frac{(1+\tau)\varepsilon}{\tau\sigma_{ns}} = \left[ (G_M^p(Q^2))^2 + \frac{\varepsilon}{\tau} (G_E^p(Q^2))^2 \right], \quad (2)$$

where  $\sigma_{ns}$  is the non-structure cross section,  $\varepsilon$  is the virtual photon longitudinal polarization parameter defined as  $\varepsilon^{-1} = \left[ 1 + 2(1+\tau)\tan^2(\frac{\theta_e}{2}) \right]$ , and  $\theta_e$  is the electron scattering angle.

Equation (2) is known as the Rosenbluth formula [2] or the Longitudinal-Transverse (LT) separation method. It is derived in the Born approximation based on the assumption that the electron and proton interact through the exchange of one photon (OPE). The reduced cross section  $\sigma_R$  is measured at several  $\varepsilon$  points for a fixed  $Q^2$ , and a linear fit of  $\sigma_R$  to  $\varepsilon$  gives  $(G_M^p)^2$  as the intercept and  $(G_E^p)^2/\tau$  as the slope allowing for the ratio  $R = G_E^p/G_M^p$  to be determined at that fixed  $Q^2$  point.

The ratio  $G_E^p/G_M^p$  can also be determined using the recoil polarization or polarized target (PT) method [3–5], which requires measurement of the spin-dependent cross section. A longitudinally polarized beam of electrons is scattered elastically, transferring their polarization to the

unpolarized protons (target). The two polarization transfer observables of interest here are the transverse,  $P_t$ , and longitudinal,  $P_l$ , components of the transferred polarization. The normal component,  $P_n$ , does not exist in elastic scattering in OPE. Simultaneous measurements of  $P_t$  and  $P_l$  allows for the determination of the ratio  $R$  as

$$R = \frac{G_E^p}{G_M^p} = -\frac{P_t(E+E')}{P_l} \frac{1}{2M_p} \tan\left(\frac{\theta_e}{2}\right), \quad (3)$$

where  $E$ ,  $E'$ , and  $\theta_e$  are the incident energy, final energy, and scattered angle of the electron.

The two methods yield strikingly different results [6–8], with values of  $\mu_p G_E^p/G_M^p$  differing almost by a factor of three at high  $Q^2$ . Here  $\mu_p$  is the magnetic moment of the proton. In the LT separation method, the ratio shows approximate form factor scaling,  $\mu_p G_E^p/G_M^p \approx 1$ , albeit with large uncertainties at high  $Q^2$  values. The recoil polarization method yields a ratio that decreases roughly linearly with increasing  $Q^2$ , with some hint of flattening out above 5 (GeV/c)<sup>2</sup>.

## II. TWO-PHOTON EXCHANGE CONTRIBUTIONS

To reconcile these measurements, several studies suggested that missing higher order radiative corrections to the electron-proton elastic scattering cross sections, in particular two-photon exchange (TPE) diagrams, may explain the discrepancy [9–11]. We account for TPE contributions to  $\sigma_R$  by adding the real function  $F(\varepsilon, Q^2)$  to the Born reduced cross section

$$\sigma_R = (G_M^p)^2 \left[1 + \frac{\varepsilon}{\tau} R^2\right] + F(\varepsilon, Q^2), \quad (4)$$

where  $R = G_E^p/G_M^p$  is the recoil polarization ratio. The role of TPE effects was studied extensively both theoretically [12–39] and phenomenologically [9, 40–52]. Most calculations suggested that the TPE corrections are relatively small, but have a significant angular dependence which mimics the effect of a larger value of  $G_E^p$ . Detailed reviews of the role of the TPE effect in electron-proton scattering can be found in [53, 54].

Experimentally, several measurements were performed to verify the discrepancy [6, 55] and to try and measure or constrain TPE contributions. Precise examinations of the  $\varepsilon$  dependence of  $\sigma_R$  [40, 41, 44] found no deviation from the linear behaviour predicted in the OPE approximation. Another measurement was performed to look for TPE effects by extracting  $\mu_p G_E^p/G_M^p$  at fixed  $Q^2$  as a function of scattering angle [56]. In the Born approximation, the result should be independent of scattering angle, and no deviation from the OPE prediction was observed.

Based on the observations above, it is possible to try and extract the TPE contributions based on the observed discrepancy between the LT and PT results. Assuming that the TPE contributions are linear in  $\varepsilon$  and that the

PT results do not depend on  $\varepsilon$ , and knowing that the TPE contribution must vanish in the forward limit ( $\varepsilon \rightarrow 1$ ) [44, 47], it is possible to extract the TPE contribution to the unpolarized cross section in a combined analysis of LT and PT data [9, 40–52]. Where polarization data exist as a function of  $\varepsilon$ , it is possible to attempt to extract the TPE amplitudes with fewer assumptions [43, 46], though with relatively large uncertainties.

The most direct technique for measuring TPE is the comparison of electron-proton and positron-proton scattering. This is done by measuring the ratio  $R_{e^+e^-}(\varepsilon, Q^2) = \frac{1-\delta_{2\gamma}}{1+\delta_{2\gamma}} \approx 1 - 2\delta_{2\gamma}$  after correcting for the electron-proton Bremsstrahlung interference term and the conventional charge-independent radiative corrections. Here  $\delta_{2\gamma}$  is the fractional TPE correction for electron-proton scattering. The leading TPE contribution comes from the interference of the OPE and TPE amplitudes, and so has the opposite sign for positron and electron scattering. The only other first-order radiative correction which depends on the lepton sign is the interference between diagrams with Bremsstrahlung from the electron and proton, and this contribution is generally small. Thus, after correcting the measured ratio for the Bremsstrahlung interference term, the comparison of positron and electron scattering allows for the most direct measurement of TPE contributions. Until recently, there was only limited evidence for any non-zero TPE contribution from such comparisons [57], as data were limited to low  $Q^2$  or large  $\varepsilon$ , where the TPE contributions appear to be small. In addition, the details of the radiative corrections applied to these earlier measurements are not always available, and it is not clear if the charge-even corrections were applied in all cases. New measurements [58, 59] have found more significant indications of TPE contributions at low  $\varepsilon$  and moderate  $Q^2$ , which are consistent with hadronic TPE calculations [13].

To account for the exchange of two or more photons, Guichon and Vanderhaeghen [9] expressed the hadronic vertex function in terms of three independent complex amplitudes (generalized form factors) which depend on both  $Q^2$  and  $\varepsilon$ :  $\tilde{G}_E^p(\varepsilon, Q^2)$ ,  $\tilde{G}_M^p(\varepsilon, Q^2)$ , and  $\tilde{F}_3(\varepsilon, Q^2)$ . These generalized form factors can be broken into the usual Born (OPE) and the TPE contributions as:  $\tilde{G}_{E,M}^p(\varepsilon, Q^2) = G_{E,M}^p(Q^2) + \delta G_{E,M}^p(\varepsilon, Q^2)$  with  $Y_{2\gamma}(\nu, Q^2)$  defined as  $\Re\left(\frac{\nu \tilde{F}_3}{M_p^2 |\tilde{G}_M^p|}\right)$ , where  $\Re$  stands for the real part, and  $\nu = M_p^2 \sqrt{(1+\varepsilon)/(1-\varepsilon)} \sqrt{\tau(1+\tau)}$ . In the Born approximation,  $\tilde{G}_{E,M}^p(\varepsilon, Q^2) = G_{E,M}^p(Q^2)$ , which are the real electric and magnetic Sachs form factors and  $\tilde{F}_3 = 0$ . With the inclusion of the TPE effects, the reduced cross section can be expressed as

$$\sigma_R = |\tilde{G}_M^p|^2 \left[1 + \frac{\varepsilon}{\tau} \frac{|\tilde{G}_E^p|^2}{|\tilde{G}_M^p|^2} + 2\varepsilon \left(1 + \frac{|\tilde{G}_E^p|}{\tau |\tilde{G}_M^p|}\right) Y_{2\gamma}\right], \quad (5)$$

and the ratio of the transverse,  $P_t$ , to the longitudinal,

$P_l$ , components of the recoil proton polarization as

$$\frac{P_t}{P_l} = -\sqrt{\frac{2\varepsilon}{\tau(1+\varepsilon)}} \left[ \frac{|\tilde{G}_E^p|}{|\tilde{G}_M^p|} + \left( 1 - \frac{2\varepsilon}{1+\varepsilon} \frac{|\tilde{G}_E^p|}{|\tilde{G}_M^p|} \right) Y_{2\gamma} \right], \quad (6)$$

allowing for the proton form factor ratio to be written for the L-T separation (Rosenbluth) as

$$R_{LT}^2 = \left( \frac{|\tilde{G}_E^p|}{|\tilde{G}_M^p|} \right)^2 + 2 \left( \tau + \frac{|\tilde{G}_E^p|}{|\tilde{G}_M^p|} \right) Y_{2\gamma}, \quad (7)$$

and for the recoil-polarization as

$$R_{PT} = \frac{|\tilde{G}_E^p|}{|\tilde{G}_M^p|} + \left( 1 - \frac{2\varepsilon}{1+\varepsilon} \frac{|\tilde{G}_E^p|}{|\tilde{G}_M^p|} \right) Y_{2\gamma}. \quad (8)$$

Phenomenologically and based on the formalism of Guichon and Vanderhaeghen, Eqs. (5) and (6), Guttman and collaborators [46] determined the  $\varepsilon$  dependence of the TPE amplitudes around  $Q^2 = 2.50$  (GeV/c)<sup>2</sup> using the high precision data on the ratios  $-\mu_p \sqrt{\tau(1+\varepsilon)/(2\varepsilon)} P_t/P_l$  and  $P_l/P_l^{\text{Born}}$  determined by the GEp-2 $\gamma$  experiment [56], and the reduced cross sections  $\sigma_R$  from the Super-Rosenbluth experiment [6]. For convenience, the reduced cross section  $\sigma_R/G_{Mp}^2$ , the ratio  $-\mu_p \sqrt{\tau(1+\varepsilon)/(2\varepsilon)} P_t/P_l$ , and the ratio  $P_l/P_l^{\text{Born}}$  were expressed in terms of the ratio  $G_E^p/G_M^p$  and the real parts of the TPE amplitudes relative to the magnetic form factor or:  $Y_M(\varepsilon, Q^2) = \Re(\delta\tilde{G}_M^p/G_M^p)$ ,  $Y_E(\varepsilon, Q^2) = \Re(\delta\tilde{G}_E^p/G_M^p)$ , and  $Y_3(\varepsilon, Q^2) = (\nu/M_p^2)\Re(\tilde{F}_3/G_M^p)$  as

$$\frac{\sigma_R}{(G_M^p)^2} = 1 + \frac{\varepsilon}{\tau} \left( \frac{G_E^p}{G_M^p} \right)^2 + 2Y_M + \frac{2\varepsilon}{\tau} \frac{G_E^p}{G_M^p} Y_E + 2\varepsilon \left( 1 + \frac{G_E^p}{\tau G_M^p} \right) Y_3 + O(e^4), \quad (9a)$$

$$-\sqrt{\frac{\tau(1+\varepsilon)}{2\varepsilon}} \frac{P_t}{P_l} = \frac{G_E^p}{G_M^p} + Y_E - \frac{G_E^p}{G_M^p} Y_M + \left( 1 - \frac{2\varepsilon}{1+\varepsilon} \frac{G_E^p}{G_M^p} \right) Y_3 + O(e^4), \quad (9b)$$

$$\begin{aligned} \frac{P_l}{P_l^{\text{Born}}} &= 1 - 2\varepsilon \left( 1 + \frac{\varepsilon}{\tau} \left( \frac{G_E^p}{G_M^p} \right)^2 \right)^{-1} \\ &\times \left\{ \left[ \frac{\varepsilon}{1+\varepsilon} \left( 1 - \frac{1}{\tau} \left( \frac{G_E^p}{G_M^p} \right)^2 \right) + \frac{G_E^p}{\tau G_M^p} \right] Y_3 \right. \\ &\left. + \frac{G_E^p}{\tau G_M^p} \left[ Y_E - \frac{G_E^p}{G_M^p} Y_M \right] \right\} + O(e^4). \quad (9c) \end{aligned}$$

The ratio  $-\mu_p \sqrt{\tau(1+\varepsilon)/(2\varepsilon)} P_t/P_l$  does not show any  $\varepsilon$  dependence and a fit in the form of:  $\mu_p R + B\varepsilon^c(1-\varepsilon)^d$  was performed. Here  $\mu_p R = \mu_p G_E^p/G_M^p$  is the Born value (OPE), with  $B$ ,  $c$ , and  $d$  being constants. For several values of  $c$ , and  $d$ , the constant  $B$  was effectively zero, and the ratio  $P_t/P_l$  was fit to its Born value of  $\mu_p R = \mu_p G_E^p/G_M^p = 0.693 \pm 0.006_{\text{stat}} \pm 0.010_{\text{sys}}$ . The

ratio  $P_l/P_l^{\text{Born}}$  shows a decrease for  $\varepsilon \rightarrow 0$ . Although in qualitative agreement with perturbative QCD (pQCD) [16, 29], the ratio  $P_l/P_l^{\text{Born}}$  at  $Q^2 = 2.50$  (GeV/c)<sup>2</sup> falls-off faster than the pQCD prediction. Therefore, the ratio  $P_l/P_l^{\text{Born}}$  was fit to two different functional forms:  $P_l/P_l^{\text{Born}} = 1 + a_l \varepsilon^4 (1-\varepsilon)^{1/2}$  (Fit I), and  $P_l/P_l^{\text{Born}} = 1 + a_l \varepsilon \ln(1-\varepsilon)(1-\varepsilon)^{1/2}$  (Fit II), giving a value of  $a_l = 0.11 \pm 0.03_{\text{stat}} \pm 0.06_{\text{sys}}$  for (Fit I), and  $a_l = -0.032 \pm 0.008_{\text{stat}} \pm 0.020_{\text{sys}}$  for (Fit II). To find the  $\varepsilon$  dependence of  $\sigma_R$  at  $Q^2 = 2.64$  (GeV/c)<sup>2</sup> and due to the experimentally observed linearity of the Rosenbluth plots, a fit of  $\sigma_R/(\mu_p G_D)^2$  to  $\varepsilon$  using the form  $(a + b\varepsilon)$  was done. Here  $G_D(Q^2)$  is the dipole parametrization:  $G_D(Q^2) = [1 + Q^2/(0.71(\text{GeV}/c)^2)]^{-2}$ . This fit yields a value of  $a = 1.106 \pm 0.006$  and  $b = 0.160 \pm 0.009$ . Using the assumption that for  $\varepsilon \rightarrow 1$ , Regge limit, the TPE correction to  $\sigma_R$  vanishes,  $\sigma_R$  can now be expressed in the OPE approximation as:  $\sigma_R/(\mu_p G_D)^2 = [(G_M^p)^2 + (G_E^p)^2/\tau]/(\mu_p G_D)^2 = (a + b)$ . Using the obtained values of  $a$ ,  $b$ , and  $\mu_p R = \mu_p G_E^p/G_M^p$ , the ratio  $(G_M^p/\mu_p G_D)^2$  was found to be  $(G_M^p/\mu_p G_D)^2 = 1.168 \pm 0.010$ .

Using the  $\varepsilon$ -dependence forms obtained for  $\sigma_R/(G_M^p)^2$ ,  $-\mu_p \sqrt{\tau(1+\varepsilon)/(2\varepsilon)} P_t/P_l$ , and  $P_l/P_l^{\text{Born}}$  along with the values extracted for  $(G_M^p/\mu_p G_D)^2$  and  $\mu_p R = \mu_p G_E^p/G_M^p$  in Eqs. (9), the three TPE amplitudes  $Y_M$ ,  $Y_E$ , and  $Y_3$  were extracted as a function of  $\varepsilon$  at  $Q^2 = 2.50$  (GeV/c)<sup>2</sup>. The amplitude  $Y_M$  is on the few percent level and is mainly driven by the TPE effect in  $\sigma_R$  which is to a good approximation given by  $\sigma_R^{2\gamma} \sim (Y_M + \varepsilon Y_3)$ . The amplitude  $Y_M$  rises approximately linearly in  $\varepsilon$  and starts showing deviation from linearity as  $\varepsilon \rightarrow 1$ . On the other hand, the amplitudes  $Y_E$  and  $Y_3$  are mainly driven by the polarization data. They are on the 2-3% level and have opposite signs in the region constrained by the polarization data ( $\varepsilon \geq 0.6$ ). Therefore, they tend to partially cancel each other in the polarization transfer ratio. The leading TPE correction to the ratio  $P_t/P_l$  is approximately given by  $(P_t/P_l)^{2\gamma} = (Y_E + Y_3)$ . Finally, the amplitude  $Y_3$  is driven by the  $P_l$  data and the TPE correction to  $P_l$  is given by  $P_l^{2\gamma} \approx -2\varepsilon^2/(1+\varepsilon)Y_3$ .

Based on the framework of [9], Arrington [45] performed a global analysis where he extracted the TPE amplitudes  $\Delta G_{E,M}^p$  and  $Y_{2\gamma}$ . He assumed that the amplitudes were  $\varepsilon$ -independent and took  $\Delta G_E^p = 0$ . Values for  $Y_{2\gamma}(Q^2)$  were extracted from the difference between polarization and Rosenbluth measurements, taking into account the uncertainties in both data sets. Based on the high- $\varepsilon$  constraints from the comparison of positron and electron scattering [57] the amplitude  $\Delta G_{Mp}$  was determined by requiring that its contribution to  $\sigma_R$  at  $\varepsilon = 1$  cancelled the contribution of  $Y_{2\gamma}$ . The extracted TPE amplitudes and their estimated uncertainties are then parametrized as a function of  $Q^2$ , and used to apply TPE corrections to the form factors obtained from a global Rosenbluth analysis [11] and the new recoil polarization data. The  $Y_{2\gamma}$  amplitude was determined in the range of  $0.6 \leq Q^2 \leq 6$  (GeV/c)<sup>2</sup> and then parametrized

according to:  $Y_{2\gamma} = 0.035[1 - \exp(-Q^2/1.45)]$ . In contrast to [9], the true ratio  $G_E^p/G_M^p$  obtained was actually corrected for all TPE amplitudes  $\delta G_{E,M}^p$  and  $Y_{2\gamma}$  and it was well parametrized by  $\mu_p G_E^p/G_M^p = (1 - 0.158Q^2)$ .

In both of these analysis, there is not enough information to directly determine the amplitudes, so assumptions have to be made about the relative importance and the  $\varepsilon$  dependence of the three TPE amplitudes. Common to these analyses are the assumption that the correction is close to linear in  $\varepsilon$ , as no non-linearities have been observed [25, 40, 41, 44]. If one also neglects the TPE correction to the polarization data, which is significantly smaller at high  $Q^2$ , then it is not necessary to work in terms of the polarization amplitude; one can simply parametrize the TPE contributions to the reduced cross section, taking a linear (or nearly linear)  $\varepsilon$  dependence.

The analysis of Borisjuk and Kobushkin [43] takes a similar approach, although they use a different linear combination of amplitudes than Ref. [9]. Again, the  $\varepsilon$  dependence of  $P_t/P_l$  is taken to be zero [56], and the correction to the cross section is taken to be linear [41]. Data from available electron-proton scattering cross sections in the range of  $2.20 \leq Q^2 \leq 2.80$  (GeV/c)<sup>2</sup> were interpolated to  $Q^2 = 2.50$  (GeV/c)<sup>2</sup> to extract the amplitudes at a fixed  $Q^2$  value. This yields an extraction in terms of a single amplitude.

Theoretically, different approaches were adapted to calculate TPE corrections to electron-proton scattering observables such as: the hadronic [9, 12–15, 20, 21, 26, 27, 30–35], partonic models (GPDs) [22, 23], dispersion relations (DRs) [19, 28], and pQCD [16–18, 29, 39] based calculations. However, calculations of the TPE amplitudes or generalized form factors were done mainly using hadronic- and pQCD-based calculations. In the hadronic approach, which is mainly valid at small to moderate  $Q^2$  values, the TPE processes are mediated by the production of virtual hadrons and/or hadronic resonances in the intermediate state. Therefore, the TPE amplitudes can be broken down into contributions according to the hadronic intermediate state involved such as: the elastic contributions where only a pure nucleon is considered, and inelastic contributions coming from multi-particle states such as  $p\pi$ ,  $p\pi\pi$ , and in particular, emphasis was placed on hadronic intermediate states containing the prominent  $\Delta(1232)$  resonance, Roper resonance, and  $\pi N$  (pion + nucleon). The  $\pi N$  contribution can be further split into contributions coming from different partial waves or channels such as the  $P_{33}$  channel where the  $\Delta(1232)$  resonance resides ( $\pi N$  intermediate state with quantum numbers of the  $\Delta(1232)$  resonance) as it has 100%  $\pi N$  content, and contributions from higher total angular momentum of  $J = 1/2$  and  $3/2$  (eight different channels). However, these contributions are to be viewed as the first terms of an infinite expansion of the total  $\pi N$  contribution in the intermediate state as it is not clear when such a series will eventually converge. The second is the quark approach where the nucleon is treated as system of interacting quarks (partons) in the intermediate

state with their interactions described by perturbative Quantum Chromodynamics (pQCD).

The most important and well-studied contribution in the hadronic-type approach is the elastic contribution which influences mainly the magnetic form factor. Kondratyuk *et al.* calculated the effect of adding the  $\Delta(1232)$  resonance [14] and other several light resonances [15] on the cross section. The overall effect is smaller than the elastic contribution with the  $\Delta(1232)$  resonance yielding the largest contribution, and the contributions from the other resonances partially cancelling each other.

Borisjuk and Kobushkin [30] evaluated the  $\Delta(1232)$  resonance contribution to both the cross section and the TPE amplitudes. The  $\Delta(1232)$  resonance affected mainly the generalized electric form factor ( $\delta G_E/G_M$ ), while the elastic contribution influenced mainly the magnetic form factor ( $\delta G_M/G_M$ ). The effect of the  $\Delta(1232)$  resonance was found to grow in magnitude with  $Q^2$  where it became sizable and far exceeded that of the elastic contribution at large  $Q^2$ . This implies a relatively large correction to the recoil polarization ratio  $\mu_p G_E^p/G_M^p$  at high  $Q^2$ ,  $Q^2 > 3.0$  (GeV/c)<sup>2</sup>, including both the elastic and  $\Delta$  contributions or  $\delta R = (\delta^{el} + \delta^\Delta)$  was found to be much larger than the experimentally quoted systematic uncertainty. When the correction  $\delta R$  is applied to polarization measurements, the ratio  $R$  becomes negative at  $Q^2 = 8.5$  (GeV/c)<sup>2</sup>.

The two hadronic calculations of the  $\Delta(1232)$  resonance contribution discussed above assumed zero-width for the resonances (widths assumed negligibly small). Such an assumption is rather strong as the width of the  $\Delta(1232)$  resonance ( $\Gamma_\Delta \approx 110$  MeV) is comparable to the distance from threshold ( $M_\Delta \approx 160$  MeV).

Borisjuk and Kobushkin [31] evaluated the effect of the  $\pi N$  (pion + nucleon) hadronic intermediate state with emphasis on the  $P_{33}$  channel where the  $\Delta(1232)$  resonance resides. They included a realistic resonance width and shape and corresponding background. While the  $\Delta(1232)$  resonance contribution is negligible compared to the elastic one at low  $Q^2$ , the correction to the  $\delta G_E/G_M$  amplitude is large and grows rapidly in magnitude for  $Q^2 \geq 2.50$  exceeding that of the elastic intermediate state in agreement with their previous results which assumed zero-width [30]. Consequently, the recoil polarization ratio  $\mu_p G_E^p/G_M^p$  is affected at high  $Q^2$ . However, the magnitude of the correction is  $\sim 30\%$  smaller than that obtained assuming zero-width.

Calculations of the TPE amplitudes taking into account hadronic intermediate state containing the  $\pi N$  system with higher total angular momentum ( $J = 1/2$  and  $3/2$  for eight  $\pi N$  different channels) assuming finite resonance width, realistic resonance shape and form factors, as well as nonresonant background were also performed [32]. It was found that the largest contributions came from the channels with quantum numbers of the lightest resonances dominated mainly by the contribution of the  $P_{33}$  channel. On the other hand, the cor-

rection to the recoil polarization ratio  $\delta R$  at high  $Q^2$  is smaller but still sizable and grows roughly linearly with  $Q^2$  due to a cancellation between the different channels contributions.

Zhou and Yang [34, 35] calculated the  $\Delta(1232)$  resonance contribution to  $\sigma_R$  where they used a correct vertex function for  $\gamma N \rightarrow \gamma N \Delta$ , realistic  $\gamma N \Delta$  form factors, and coupling constants. In their calculations, the TPE correction  $\delta_\Delta$  showed a rising and decreasing behaviour as  $\varepsilon \rightarrow 1$  in disagreement with predictions of other hadronic calculations which suggested the vanishing of the correction in the limit  $\varepsilon \rightarrow 1$ . Such disagreement was attributed to the asymptotic behaviour of the TPE amplitudes at  $s \rightarrow \infty$  which was assumed to vanish in other calculations. While their calculations agreed reasonably well with measured  $\sigma_R$  from Ref. [60], substantial discrepancy remained when  $\sigma_R$  data from Refs. [6, 61] were used. They concluded that their model should be restricted to low energy,  $W \leq 3\text{--}4$  GeV, and to low  $Q^2$  experimental data in that energy range.

Lorenz *et al.* [21] calculated TPE corrections to  $\sigma_R$  including elastic and  $\Delta$ -resonance intermediate states using phenomenological information on the vertices. They included Coulomb contribution and updated photocoupling values for the  $\gamma N \delta$ -vertices, and used data on the  $Q^2$  dependence of the nucleon- $\Delta$  transition from electroproduction of nucleon resonances in terms of helicity amplitudes. The results showed strong dependence on the choice of elastic nucleon and nucleon- $\Delta$  transition form factors used as input, in disagreement with previous calculations. At low  $Q^2$ , the  $\Delta$  contribution is much smaller than the elastic contribution. On the other hand, the contribution at high  $Q^2$  is comparable to that of the elastic.

At high  $Q^2$  values, the hadronic approach becomes inadequate and the TPE corrections are calculated mainly within the framework of GPDs [22, 23] and pQCD [16–18, 29, 39]. Afanasev *et al.* [23] calculated TPE corrections to  $\sigma_R$  using formalism of GPDs. The authors doubt the applicability of pQCD for the currently existing data. Borisyyuk and Kobushkin [29] calculated TPE corrections to  $\sigma_R$  (the  $\delta G_M/G_M$  amplitude) within the framework of pQCD for the proton target using wave functions based on QCD sum rules. The  $\delta G_M/G_M$  amplitude has linear  $\varepsilon$  dependence, and grows logarithmically with  $Q^2$  reaching 3.5% of the Born amplitude at  $Q^2 = 30$  (GeV/c)<sup>2</sup>. At lower  $Q^2$ , a smooth connection with hadronic calculations assuming an elastic intermediate state is possible. However, at high  $Q^2$ , the two calculations yield different results suggesting the inadequacy of the hadronic approach for  $Q^2 \geq 3.0$  (GeV/c)<sup>2</sup>. Kivel and Vanderhaeghen [18] calculated TPE corrections to  $\sigma_R$  at moderately large  $Q^2$  values of 2.64, 3.20, and 4.10 (GeV/c)<sup>2</sup> using a QCD factorization approach within the framework of the soft-collinear effective theory (SCET) arising from both the soft- and hard-spectator scattering contributions. The TPE corrections to  $\sigma_R$  are linear in  $\varepsilon$  but small in magnitude. However, for  $Q^2 > 2.5\text{--}3.0$  (GeV/c)<sup>2</sup>, the descrip-

tion of  $\sigma_R$  as a linear function in  $\varepsilon$  for the whole  $\varepsilon$  range is no longer valid as deviation from linearity at small  $\varepsilon$  is seen at large  $Q^2$ . While the effect of nonlinearity is relatively small at  $Q^2 = 2.64$  (GeV/c)<sup>2</sup>, it is sizable at  $Q^2 = 4.10$  (GeV/c)<sup>2</sup>. Such observation is also in agreement with hadronic-type calculations which reported similar behaviour at moderate  $Q^2$  values. The TPE amplitudes  $Y_M$  and  $Y_3$  were also calculated and both showed weak  $Q^2$  dependence with opposite  $\varepsilon$  dependence. The absolute values of the amplitudes are much smaller than those extracted phenomenologically in Ref. [46] and with non-vanishing value as  $\varepsilon \rightarrow 1$ . The ratio  $P_l/P_l^{\text{Born}}$  is dominated by the soft-spectator contribution and with non-vanishing value at  $\varepsilon = 1$ .

### III. EXTRACTION OF THE TPE AMPLITUDES

In this section I discuss the procedure used to extract the three TPE amplitudes  $Y_M$ ,  $Y_E$ , and  $Y_3$  (generalized form factors) as a function of  $\varepsilon$  at fixed  $Q^2$  value based on the formalism of Guichon and Vanderhaeghen, Eqs. (9). The procedure followed by Guttmann *et al.* [46] to extract the  $\varepsilon$  dependence of the TPE amplitudes at  $Q^2 = 2.50$  (GeV/c)<sup>2</sup> was outlined in Sec.(II). They used the measurements of the  $\varepsilon$  dependence of the ratios  $\mu_p R$  and  $P_l/P_l^{\text{Born}}$  at  $Q^2 = 2.50$  (GeV/c)<sup>2</sup> from Ref. [56], along with the  $\varepsilon$  dependence of the cross section at  $Q^2 = 2.64$  (GeV/c)<sup>2</sup> from Ref. [6] to constrain the three TPE amplitudes. However, the parametrizations of the  $\varepsilon$  dependence of the ratio  $P_l/P_l^{\text{Born}}$  used in their analysis, Fits I and II, are not well motivated by the experimental data.

In this article I do the following:

(i) I show in principle that the TPE amplitudes under certain assumptions and constraints can be extracted at fixed  $Q^2$  value using combined cross section and polarization measurements of elastic electron-proton scattering.

(ii) I extend the previous extractions [46] to cover both low- and high- $Q^2$  values, and provide simple parametrizations of the TPE amplitudes. I compare my results to different phenomenological extractions and direct TPE calculations.

(iii) I use my parametrizations of the TPE amplitudes to calculate the ratio  $P_l/P_l^{\text{Born}}$  for a range of low- and high- $Q^2$  values, and then compare the results to recent fits, theoretical calculations, and direct measurements at  $Q^2 = 2.50$  (GeV/c)<sup>2</sup>.

The procedure, together with the constraints and assumptions used is outlined below:

(1) I assume that the TPE correction is responsible mainly for the discrepancy between the cross section and polarization data measurements.

(2) Because the recoil polarization data were confirmed “*experimentally*” to be essentially independent of  $\varepsilon$ , I constrain the ratio  $-\sqrt{\tau(1+\varepsilon)}/(2\varepsilon)P_t/P_l$  in Eq. (9b) to its  $\varepsilon$ -independent term (Born value) or  $R = G_E^p/G_M^p$  by setting the TPE contributions to zero. Therefore, I will

use the recent improved parametrization of the ratio  $R$  along with its associated uncertainty [52] from polarization measurements at both low- and high- $Q^2$  values

$$\mu_p R = \frac{1}{1 + 0.1430Q^2 - 0.0086Q^4 + 0.0072Q^6}, \quad (10)$$

with an absolute uncertainty in the fit given by:  $\delta_R^2(Q^2) = \mu_p^{-2}[(0.006)^2 + (0.015\ln(1 + Q^2))^2]$ , with  $Q^2$  in  $(\text{GeV}/c)^2$ . Therefore, the amplitude  $Y_M(\varepsilon, Q^2)$  can be expressed in terms of the remaining  $Y_E(\varepsilon, Q^2)$  and  $Y_3(\varepsilon, Q^2)$  amplitudes as

$$Y_M(\varepsilon, Q^2) = \frac{Y_E(\varepsilon, Q^2) + \left(1 - \frac{2\varepsilon}{1+\varepsilon}R\right)Y_3(\varepsilon, Q^2)}{R}. \quad (11)$$

(3) Using the constraint on  $Y_M(\varepsilon, Q^2)$  from Eq. (11), I can now express  $\sigma_R/(G_M^p)^2$  in Eq. (9a) in terms of the  $Y_E$  and  $Y_3$  amplitudes as

$$\frac{\sigma_R}{(G_M^p)^2} = 1 + \frac{\varepsilon}{\tau}R^2 + \left[\frac{2}{R} + \frac{2\varepsilon R}{\tau}\right]Y_E(\varepsilon, Q^2) + \left[\frac{2}{R}\left(1 - \frac{2\varepsilon R}{1+\varepsilon}\right) + 2\varepsilon\left(1 + \frac{R}{\tau}\right)\right]Y_3(\varepsilon, Q^2). \quad (12)$$

(4) Because the TPE amplitudes are functions of  $\varepsilon$  and  $Q^2$ , I expand each of the amplitudes  $Y_E$  and  $Y_3$  as a polynomial of degree  $n$  as

$$Y_E(\varepsilon, Q^2) = \sum_{k=0}^n \alpha_k(Q^2)\varepsilon^k, \\ Y_3(\varepsilon, Q^2) = \sum_{k=0}^n \beta_k(Q^2)\varepsilon^k, \quad (13)$$

where the coefficients  $\alpha_k$  and  $\beta_k$  ( $k = 0, 1, \dots, n$ ) are functions of  $Q^2$  only.

(5) Because of the experimentally observed linearity of the Rosenbluth plots [25, 40, 41, 44] where  $\sigma_R$  exhibits no (or weak) nonlinearity in  $\varepsilon$ , I truncate the series at  $n = 2$  to reserve as possible the linearity of  $\sigma_R$  as well as to account for any possible nonlinearities in the TPE amplitudes

$$Y_E(\varepsilon, Q^2) = \alpha_0 + \alpha_1\varepsilon + \alpha_2\varepsilon^2,$$

and

$$Y_3(\varepsilon, Q^2) = \beta_0 + \beta_1\varepsilon + \beta_2\varepsilon^2. \quad (14)$$

(6) Substituting Eqs. (14) in Eq. (9a), and imposing the Regge limit where the TPE correction to  $\sigma_R$  vanishes in the limit  $\varepsilon \rightarrow 1$ , I obtain  $Y_E(1, Q^2) = -Y_3(1, Q^2)$  or simply:  $(\alpha_0 + \alpha_1 + \alpha_2) = -(\beta_0 + \beta_1 + \beta_2)$ . Further, to ensure the correct behaviour of the TPE amplitudes as  $\varepsilon \rightarrow 1$  where each amplitude must go to zero (Regge limit), I obtain the following constraints on the coefficients:  $\alpha_0 = -(\alpha_1 + \alpha_2)$  and  $\beta_0 = -(\beta_1 + \beta_2)$ .

(7) Using the constraints on  $\alpha_0$  and  $\beta_0$  derived above,  $\sigma_R$  can now be expressed as

$$\frac{\sigma_R}{(G_M^p)^2} = 1 + \frac{\varepsilon}{\tau}R^2 + \left[\frac{2}{R} + \frac{2\varepsilon R}{\tau}\right]\left[\alpha_1(\varepsilon - 1) + \alpha_2(\varepsilon^2 - 1)\right] + \left[\frac{2}{R}\left(1 - \frac{2\varepsilon R}{1+\varepsilon}\right) + 2\varepsilon\left(1 + \frac{R}{\tau}\right)\right]\left[\beta_1(\varepsilon - 1) + \beta_2(\varepsilon^2 - 1)\right] \quad (15)$$

with  $(G_M^p)^2$ ,  $\alpha_1$ ,  $\alpha_2$ ,  $\beta_1$ , and  $\beta_2$  are functions of  $Q^2$  only, and can in principle be determined by fitting  $\sigma_R$  to  $\varepsilon$  for a fixed  $Q^2$  value.

(8) In order to utilize Eq. (15) above, and for a fixed  $Q^2$  value,  $\sigma_R$  must be measured at a minimum of six  $\varepsilon$  points. However, the number of fitting parameters can be reduced by fixing the value of  $(G_M^p)^2$  and making use of the assumption that for  $\varepsilon \rightarrow 1$ , the TPE correction to  $\sigma_R$  vanishes or:  $\sigma_R(\varepsilon = 1, Q^2) = [(G_M^p)^2 + (G_E^p)^2]/\tau$ . In addition, because of the experimentally observed linearity of the Rosenbluth plots where  $\sigma_R$  data show a linear behaviour in  $\varepsilon$  suggesting the fit:  $\sigma_R = [a(Q^2) + \varepsilon b(Q^2)]$ . Therefore, for a fixed  $Q^2$  value, I linear fit  $\sigma_R$  to  $\varepsilon$  and extract the constants  $a(Q^2)$  and  $b(Q^2)$ . Equating the two expressions for  $\sigma_R(\varepsilon = 1, Q^2)$  yields

$$(G_M^p(Q^2))^2 = \frac{a(Q^2) + b(Q^2)}{\left(1 + \frac{R^2}{\tau}\right)}. \quad (16)$$

(9) I constrain  $R$  and  $(G_M^p)^2$  in Eq. (15) to their values as given by Eqs. (10) and (16), respectively, and fit  $\sigma_R$  to  $\varepsilon$  with  $\alpha_i$  and  $\beta_i$  ( $i = 1, 2$ ) being the parameters of the fit. The coefficients  $\alpha_0$  and  $\beta_0$  are then determined using the constraints:  $\alpha_0 = -(\alpha_1 + \alpha_2)$  and  $\beta_0 = -(\beta_1 + \beta_2)$ . Finally, for a fixed  $Q^2$  value, the three TPE amplitudes and the ratio  $P_l/P_l^{\text{Born}}$  are determined as a function of  $\varepsilon$  using Eqs. (11) and (14), and Eq. (9c), respectively.

#### IV. RESULTS AND DISCUSSION

I extract the values of  $(G_M^p(Q^2))^2$  and the TPE amplitudes coefficients  $\alpha_k$  and  $\beta_k$  ( $k = 1, 2$ ) following the procedure outlined in Sec. (III). I fit the world data on  $\sigma_R$  used in the analysis of Ref. [52] to extract  $(G_M^p(Q^2))^2$  first following Eq. (16). By fixing the values of  $(G_M^p(Q^2))^2$  and the recoil polarization ratio  $R$ , I then fit  $\sigma_R$  to Eq. (15), and extract the TPE amplitudes coefficients. In this analysis, 93  $Q^2$  points up to  $Q^2 = 5$   $(\text{GeV}/c)^2$  were used with  $\sigma_R$  measured at a minimum of five  $\varepsilon$  points. For the high  $Q^2$  points,  $Q^2 \gtrsim 1$   $(\text{GeV}/c)^2$ , the majority of  $\sigma_R$  measurements were made at a limited number of  $\varepsilon$  points (below 5 points), and therefore, only a handful set of these  $Q^2$  points could be used in the analysis. However, this was not the case for the low- $Q^2$  measurements.

Figure 1 shows the result of my  $\sigma_R$  fit for a sample of low- and high- $Q^2$  data points along with the Rosenbluth fit for comparison. My fit describes the data remarkably well with some deviation from linearity at low  $\varepsilon$  for the

high  $Q^2$  points. Such nonlinearity was also observed in several hadronic- and pQCD-based calculations in this range. See discussion in Sec. II for details. While most  $\sigma_R$  fits yielded reasonable reduced  $\chi^2$  values ranging from  $0.03 < \chi^2_\nu < 1.80$ , fits to 17 low- $Q^2$  data points in the range  $0.0195 < Q^2 < 0.779$  (GeV/c) $^2$  from Refs. [66, 68] yielded  $\chi^2_\nu > 1.80$ .

I also determined the values of  $(G_E^p(Q^2))^2$  using the improved parametrization of the ratio  $R$  and its associated uncertainty [52]. The values of  $(G_E^p/G_D(Q^2))^2$  and  $(G_M^p/\mu_p G_D(Q^2))^2$  along with the fit results for the TPE amplitudes coefficients are included in the online Supplemental Material [62].

Figure 2 shows the values of  $(G_E^p/G_D(Q^2))^2$  and  $(G_M^p/\mu_p G_D(Q^2))^2$  extracted from this work. I also compare my results to the values as extracted based on hadronic calculations, labeled ‘‘AMT-Hadronic’’ [63] and ‘‘VAMZ’’ [64]. In addition, I show fits from previous phenomenological analyses labeled: ‘‘ABGG’’ [65], ‘‘Bernauer’’ [66], ‘‘Arrington- $Y_{2\gamma}$ ’’ [45], and ‘‘Puckett’’ [67].

For  $(G_E^p/G_D(Q^2))^2$ , my results in general are in reasonably good agreement with extractions using calculated TPE corrections and phenomenological-based fits. However, the ‘‘Bernauer’’ and the ‘‘Arrington- $Y_{2\gamma}$ ’’ fits are very different at large  $Q^2$ . The ‘‘Arrington- $Y_{2\gamma}$ ’’ fit, on the other hand, is the only analysis that allows for TPE contributions to the recoil polarization data, though the extraction of these terms is extremely model dependent.

For  $(G_M^p/\mu_p G_D(Q^2))^2$  and at low  $Q^2$ , my results are significantly above most previous fits. This reflects the discrepancy between the recent Mainz data which yields values of  $G_M^p$  which are systematically 2–5% larger than previous world data [66]. At low  $Q^2$ , this corresponds to only a small difference in the cross section at large scattering angle, but for the larger  $Q^2$  values of the Mainz experiment, this corresponds to a significant difference in the measured cross sections. Note that except for the Bernauer result, most of the previous phenomenological extractions of the form factors and TPE contributions were focused on large  $Q^2$  values, and so did not always worry about how well the parameterizations of  $R$  reproduced low  $Q^2$  data.

The TPE amplitudes coefficients  $\alpha_k$  and  $\beta_k$  ( $k = 0, 1, 2$ ) extracted from this work as a function of  $Q^2$  are shown in Fig. 3. The coefficients are at the few-percentage-points level, and all show hints of oscillatory behaviour below  $Q^2 = 1.0$  (GeV/c) $^2$  with clear sign of structure (dips/bumps) at  $Q^2 \approx 0.02$  (GeV/c) $^2$ . For  $Q^2 \gtrsim 1.0$  (GeV/c) $^2$ , the extractions were done using a limited number of  $Q^2$  points, the coefficients change sign and increase in magnitude with increasing  $Q^2$  but with larger uncertainties.

Recently [52], the proton form factors and the TPE correction  $a(Q^2)$  values were extracted based on the parametrization from Borisyuk and Kobushkin (BK parametrization) [27] where  $\sigma_R$  is expressed in the fol-

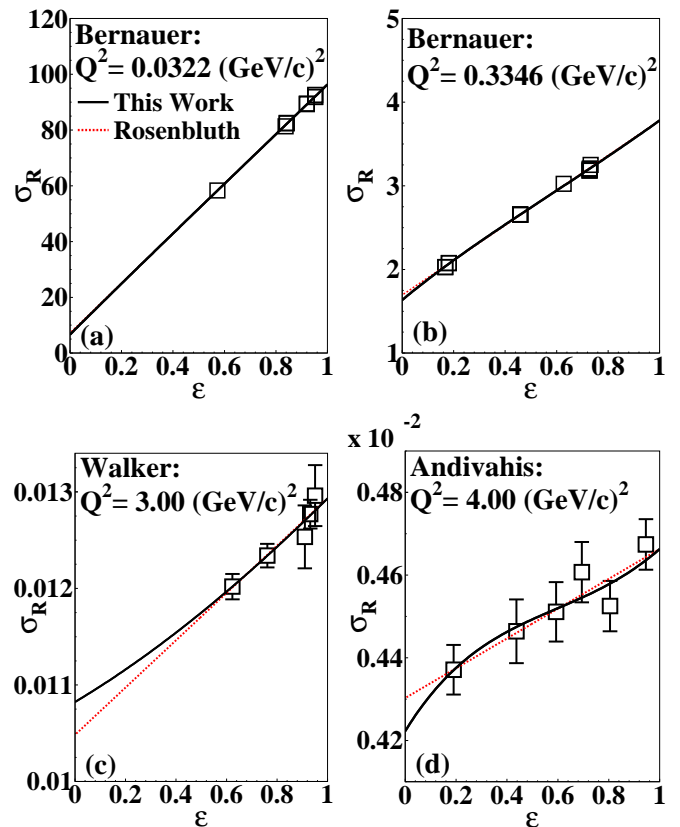


FIG. 1: (Color online) The reduced cross section  $\sigma_R$  as a function of  $\epsilon$  for a sample of low- and high- $Q^2$  data points from the data of Refs. [60, 61, 66]. Also shown my new fit based on Eq. (15) (solid black line), and the Rosenbluth fit (dashed red line) for comparison.

lowing form

$$\sigma_R = (G_M^p)^2 \left[ 1 + \frac{\epsilon}{\tau} R^2 \right] + 2a(Q^2)(1 - \epsilon)(G_M^p)^2. \quad (17)$$

While the values of the TPE parameter  $a(Q^2)$  extracted from Mainz data [66] show hints of oscillatory behaviour below  $Q^2 = 0.3$  GeV $^2$ , the uncertainties in the extracted TPE contribution are an underestimate of the true uncertainties. The quoted uncertainties on the individual cross sections do not include correlated systematic effects, which are a significant contribution to the total uncertainty in their final form factor parameterization, and I do not account for any residual uncertainty in the normalization of the data subsets which are fit as part of the global analysis [66]. So while the oscillatory behaviour in the TPE amplitudes coefficients extracted in this work seems significant compared to the uncertainties that are shown, these uncertainties are incomplete and this cannot be taken as meaningful evidence for such structure.

The TPE amplitudes coefficients are then used to construct the TPE amplitudes using Eqs. (11) and (14). Out of the 93  $Q^2$  points analyzed, 17 points yielded unex-

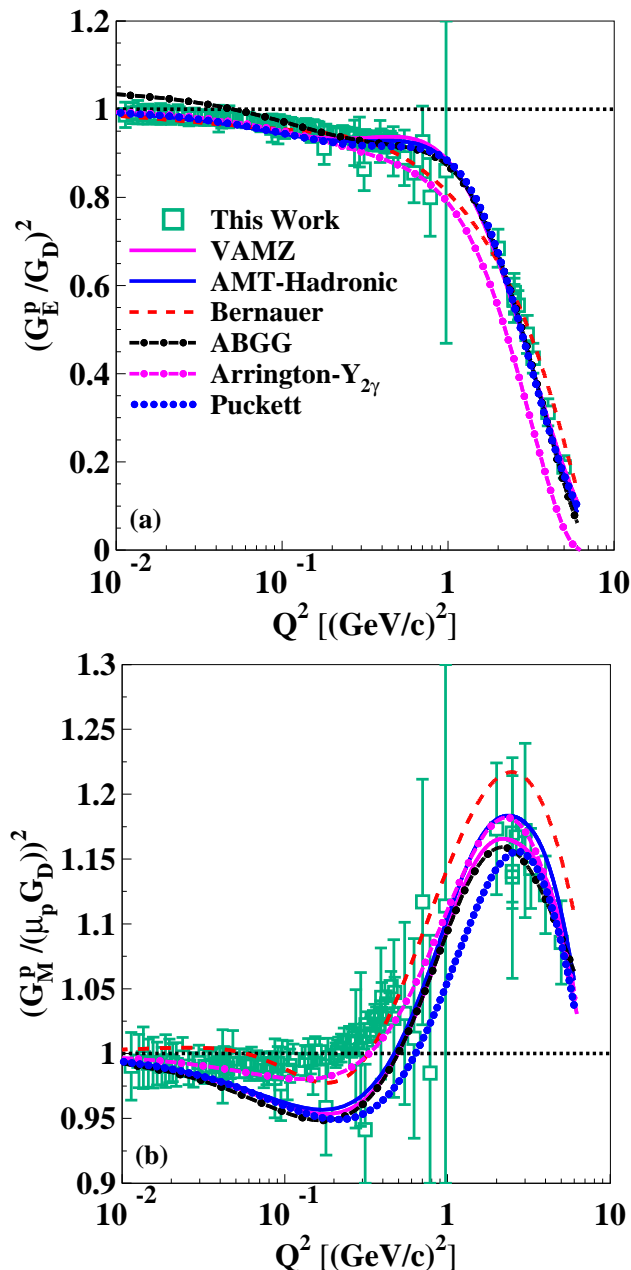


FIG. 2: (Color online)  $(G_E^p/G_D(Q^2))^2$  (top) and  $(G_M^p/\mu_p G_D(Q^2))^2$  (bottom) as obtained using Eq. (16) and the parametrization of the ratio  $R$  from Eq. (10) (Open dark-green squares). In addition, I compare the results to the extractions from several previous TPE calculations and phenomenological fits: AMT [63] (solid blue line), VAMZ [64] (solid magenta line), Bernauer [66] (long-dashed red line), ABGG [65] (dashed-dotted black line), Arrington  $Y_{2\gamma}$  [45] (dashed-dotted magenta line), and Puckett (large-dotted blue line) (the fit labeled “new” in Ref. [67]).

pectedly large TPE amplitudes exceeding the 10% level. These points are: 13 points in the range  $0.2 \leq Q^2 \leq 0.7$  (GeV/c) $^2$  from Ref. [66],  $Q^2 = 0.779$  (GeV/c) $^2$  from Ref. [68],  $Q^2 = 2.0$  (GeV/c) $^2$  from Ref. [61], and  $Q^2 = 2.5$  and  $5.0$  (GeV/c) $^2$  from Ref. [60]. Note that these

points are not shown in Fig. 3 for clarity. However, no correlation was found between the large TPE amplitudes values obtained using these  $Q^2$  points and the large  $\chi_\nu^2$  obtained from the  $\sigma_R$  fits.

In an attempt to parametrize the  $Q^2$  dependence of the TPE amplitudes coefficients  $\alpha(\beta)_{(0,1,2)}(Q^2)$ , several different functional forms were tried. All fits yielded unexpectedly large  $\chi_\nu^2$  when all the 93  $Q^2$  points were included in the fit. However, the best fits were achieved when “all” the TPE amplitudes coefficients were parametrized as a second-order polynomial of the form:  $\alpha(\beta)_{(0,1,2)}(Q^2) = (a_0 + a_1 Q^2 + a_2 Q^4)$ , and when the 17  $Q^2$  data points with large TPE amplitudes were excluded. The fits, valid up to  $Q^2 = 4$  (GeV/c) $^2$ , are shown in Fig. 3 as solid red lines, and the parameters of the fits are listed in Table I. The coefficients  $\alpha_2$  and  $\beta_2$  have the largest  $\chi_\nu^2$  values. However, calculating these two coefficients using the constraints:  $\alpha_2 = -(\alpha_0 + \alpha_1)$  and  $\beta_2 = -(\beta_0 + \beta_1)$  yielded effectively the same results as those of the fits.

The  $\varepsilon$  dependence of the TPE amplitudes as extracted from this work is shown in Fig. 4 for a range of  $Q^2$  values. The amplitudes are on the few-percentage-points level, and behave roughly linearly with increasing  $Q^2$ . The amplitude  $Y_M$  is the largest in magnitude. It is mainly positive at low  $Q^2$  and changes sign and increases in magnitude with increasing  $Q^2$  where it becomes non-linear. The amplitude  $Y_3$  is also sizable and positive at low  $Q^2$  and starts to decrease with increasing  $Q^2$ . At high  $Q^2$  values,  $Q^2 \sim 3.0$  (GeV/c) $^2$ ,  $Y_3$  changes sign and becomes negative and starts to grow in magnitude with increasing  $Q^2$  where it becomes non-linear. On the other hand, the amplitude  $Y_E$  is negligible and mainly negative at low  $Q^2$ . It starts to increase in magnitude with increasing  $Q^2$ , and then changes sign and becomes positive at  $Q^2 \sim 3.0$  (GeV/c) $^2$  where it continues to grow in magnitude and becomes non-linear.

The  $Y_E$  and  $Y_3$  amplitudes extracted in this work differ in magnitude, and certainly have opposite sign to each other as  $Q^2$  increases where they tend to partially cancel each other. This suggests that the TPE correction to  $\sigma_R$  is driven mainly by  $Y_M$  and to a lesser extent by  $Y_3$ . This is in agreement with the finding of Ref. [46] for the extraction of the TPE amplitudes at  $Q^2 = 2.50$  (GeV/c) $^2$ .

I also compare my results to several previous hadronic TPE calculations assuming different intermediate states: elastic labelled as “ $Y_M$  elastic”, “ $Y_E$  elastic”, “ $Y_3$  elastic” [28], and elastic +  $\pi N$  with spin 1/2 and 3/2 channels labelled as “ $Y_M$  spin”, “ $Y_E$  spin”, “ $Y_3$  spin” [32]. While my results for  $Y_M$  and  $Y_E$  are in reasonable qualitative agreement with previous hadronic calculations, showing the fall and rise of both amplitudes with increasing  $Q^2$ , my results for  $Y_3$  have opposite sign and deviate substantially from calculations except at  $Q^2 \sim 1.0$  (GeV/c) $^2$ .

In Fig. 5 I show the results of the  $\varepsilon$  dependence of the TPE amplitudes at  $Q^2 = 2.50$  (GeV/c) $^2$  along with the error bands, shown as very long-dashed lines, as computed using the covariance matrix of the fits. I compare

TABLE I: The values of the fit parameters for the TPE amplitudes coefficients  $\alpha_{(0,1,2)}(Q^2)$  and  $\beta_{(0,1,2)}(Q^2)$ .

Coefficient	$a_0$	$a_1$	$a_2$	$\chi^2_\nu$
$\alpha_0(Q^2)$	$(-0.89 \pm 1.27) \times 10^{-3}$	$(-1.45 \pm 0.80) \times 10^{-2}$	$(+7.75 \pm 2.59) \times 10^{-3}$	1.56
$\alpha_1(Q^2)$	$(-0.58 \pm 0.86) \times 10^{-3}$	$(+1.02 \pm 0.53) \times 10^{-2}$	$(-3.77 \pm 0.17) \times 10^{-3}$	1.36
$\alpha_2(Q^2)$	$(+1.22 \pm 0.80) \times 10^{-3}$	$(+3.95 \pm 5.47) \times 10^{-3}$	$(-3.78 \pm 1.87) \times 10^{-3}$	1.92
$\beta_0(Q^2)$	$(+3.19 \pm 1.43) \times 10^{-3}$	$(+5.53 \pm 8.30) \times 10^{-3}$	$(-5.88 \pm 2.69) \times 10^{-3}$	1.57
$\beta_1(Q^2)$	$(-2.56 \pm 0.85) \times 10^{-3}$	$(-0.02 \pm 4.98) \times 10^{-3}$	$(+1.51 \pm 1.58) \times 10^{-3}$	1.28
$\beta_2(Q^2)$	$(-1.49 \pm 0.89) \times 10^{-3}$	$(-3.93 \pm 5.85) \times 10^{-3}$	$(+3.94 \pm 2.00) \times 10^{-3}$	1.91

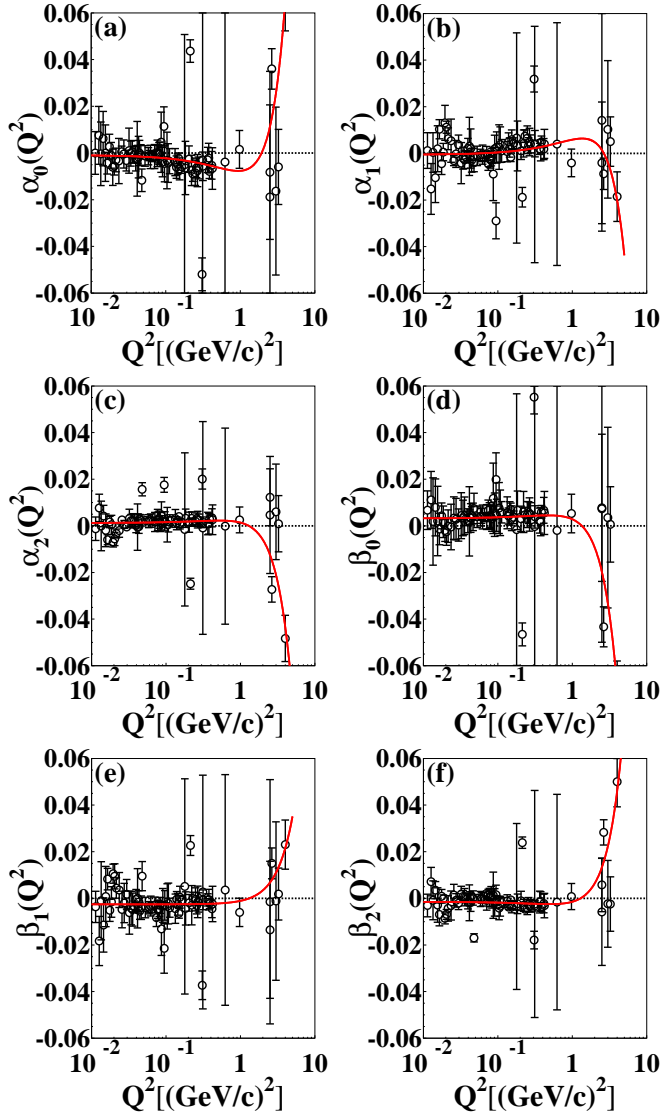


FIG. 3: (Color online) The TPE amplitudes coefficients  $\alpha_{(0,1,2)}(Q^2)$  and  $\beta_{(0,1,2)}(Q^2)$  as a function of  $Q^2$  as extracted from this work (open black circles) along with the fits (solid red lines) valid up to  $Q^2 = 4$  (GeV/c) $^2$ . Note that  $Q^2$  points which yielded large TPE amplitudes were excluded for clarity. See text for details.

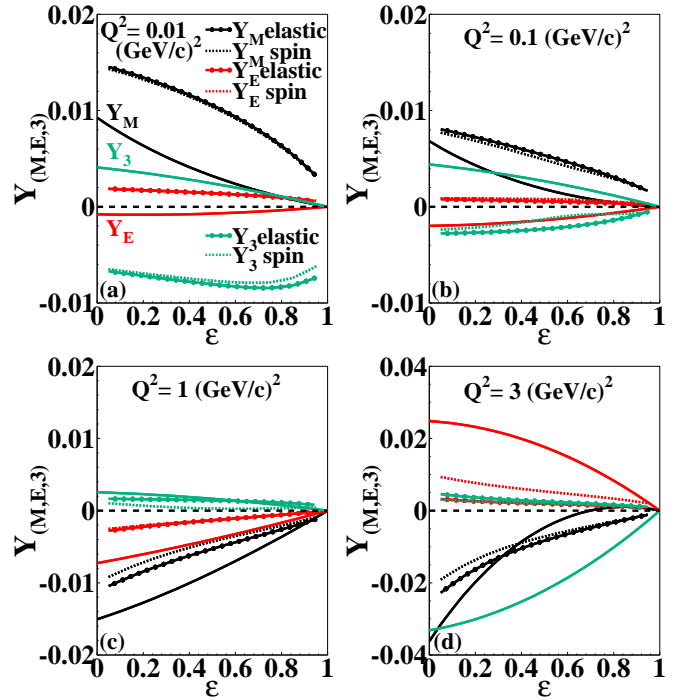


FIG. 4: (Color online) The extracted TPE amplitudes from this work:  $Y_M$  (solid black line),  $Y_E$  (solid red line) and  $Y_3$  (solid dark-green line) as a function of  $\epsilon$  at the  $Q^2$  value listed in the figure. In addition, I compare the results to previous hadronic calculations assuming different intermediate states: elastic labelled as: “ $Y_M$  elastic” (dashed-dotted black line), “ $Y_E$  elastic” (dashed-dotted red line), “ $Y_3$  elastic” (dashed-dotted dark-green line) from Ref. [28], and elastic +  $\pi N$  with spin 1/2 and 3/2 channels labelled as: “ $Y_M$  spin” (long-dashed black line), “ $Y_E$  spin” (long-dashed red line), “ $Y_3$  spin” (long-dashed dark-green line) from Ref. [32].

the results to previous phenomenological extractions of Ref. [46], labelled as “Guttmann Fit I” and “Guttmann Fit II”. In addition, I compare the results to several previous hadronic TPE calculations assuming different intermediate states: elastic “BK: elastic” [28], elastic +  $\Delta(1232)$  resonance “BK: elastic +  $\Delta(1232)$ ” [30], elastic +  $\pi N$  ( $P_{33}$  channel) “BK: elastic +  $P_{33}$ ” [31], elastic +  $\pi N$  (Spin 1/2 and 3/2 channels) “BK: elastic +  $\pi N$ ” [32],

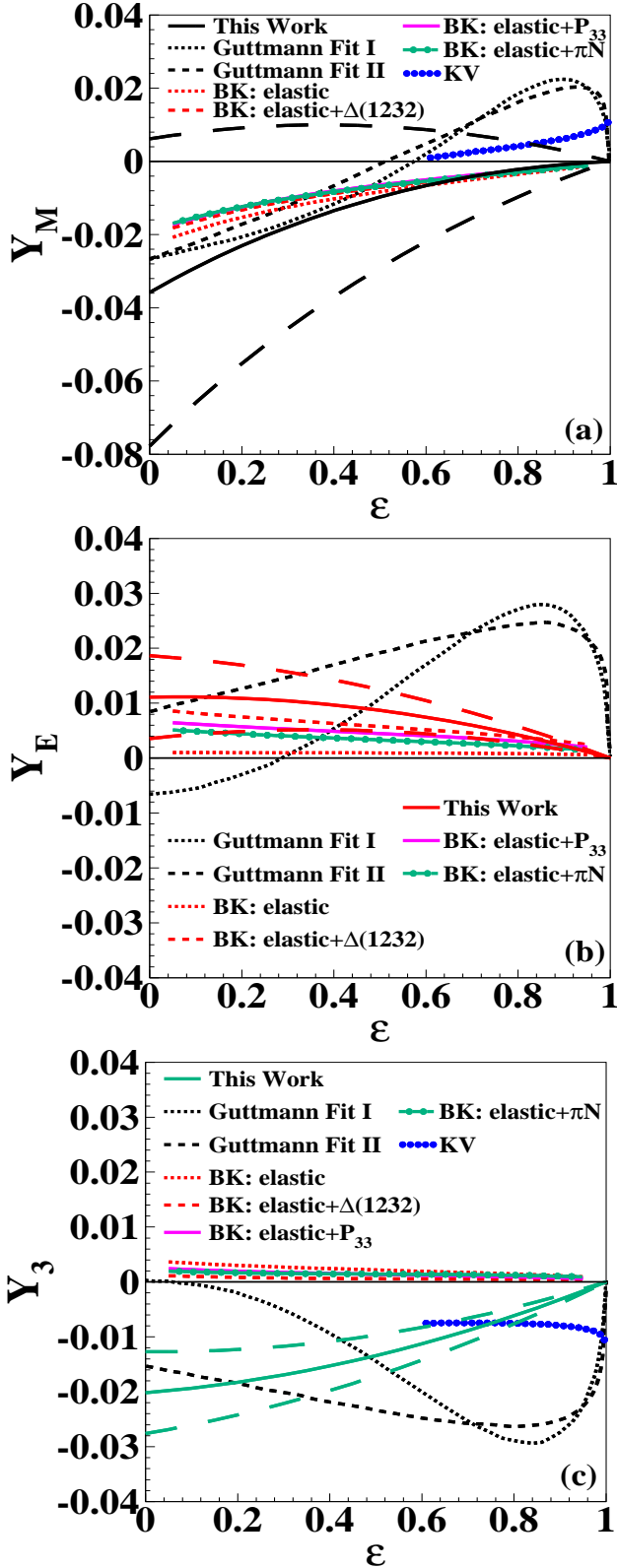


FIG. 5: (Color online) The extracted TPE amplitudes from this work:  $Y_M$  (top) (solid black line),  $Y_E$  (middle) (solid red line), and  $Y_3$  (bottom) (solid dark-green line) as a function of  $\varepsilon$  at  $Q^2 = 2.50$  (GeV/c) $^2$ . The error bands on the amplitudes are shown as very long-dashed (black, red, dark-green) lines, respectively. In addition, I compare the results to phenomenological extractions from Ref. [46] “Guttmann Fit I” (dashed black line) and “Guttmann Fit II” (long-dashed black line), and to several previous hadronic TPE predictions: “BK: elastic” [28] (dashed red line), “BK: elastic +  $\Delta(1232)$ ” [30] (long-dashed red line), “BK: elastic +  $P_{33}$ ” [31] (solid magenta line), and “BK: elastic +  $\pi N$ ” [32] (dashed-dotted dark-green line). Also shown, calculations based on QCD

factorization within the SCET approach from Ref. [18] “KV”. Note that in a leading twist QCD-type calculation, the two amplitudes  $Y_M$  and  $Y_3$  can only be calculated but not  $Y_E$  as the virtual photon (gluon) cannot flip the quark spin and calculation of the amplitude  $Y_E$  requires knowledge of the quark transverse momenta distribution.

For  $Y_M$ , and despite the large error band, my results are generally in good qualitative agreement with previous phenomenological extractions from Ref. [46] for  $\varepsilon < 0.60$ , and deviate substantially above that. On the other hand, the results are in good qualitative agreement with all hadronic TPE calculations of Refs. [28, 30–32] with the elastic contribution, “BK: elastic”, being the closest, although all hadronic calculations are very close in value with amplitudes vanishing in the limit  $\varepsilon \rightarrow 1$ . For  $Y_E$  and  $Y_3$ , the error bands are smaller and the amplitudes are more constrained than  $Y_M$ . For  $Y_E$ , my results are in very good agreement with all hadronic calculations as well with the inelastic contribution, “BK: elastic +  $\Delta(1232)$ ” being the closest, but deviate from phenomenological extractions for all  $\varepsilon$  range. For  $Y_3$ , my results disagree noticeably with both phenomenological extractions and all hadronic calculations. On the other hand, the QCD-type calculation within the SCET approach from Ref. [18] disagree strongly with my results, previous phenomenological extractions, as well as hadronic TPE predictions as the amplitudes  $Y_{(M,3)}$  do not vanish in the limit  $\varepsilon \rightarrow 1$ , with the absolute values of these amplitudes being much smaller than those obtained in Ref. [46].

Figure 6 shows the  $Q^2$  dependence of the TPE amplitudes as extracted from this work at a fixed  $\varepsilon = 0.25$ . The error bands on the amplitudes are shown as very long-dashed black lines. I also compare the results to hadronic TPE calculations arising from: elastic “BK: elastic” [28], elastic +  $\Delta(1232)$  resonance “BK: elastic +  $\Delta(1232)$ ” [30], elastic +  $\pi N$  ( $P_{33}$ ) channel “BK: elastic +  $\pi N$  ( $P_{33}$ )” [31], and elastic +  $\pi N$  (Spin 1/2 and 3/2) channels “BK: elastic +  $\pi N$  (Spin 1/2 and 3/2)” [32]. For  $Y_M$  and  $Y_E$ , although my results fall below theoretical predictions, they generally are in reasonable qualitative agreement with calculations, all showing a fall and then rise of both amplitudes with increasing  $Q^2$ . For  $Y_M$ , and at large  $Q^2$  values, the error band is large and my results are closer to calculations assuming a pure proton in the intermediate state (elastic) suggesting that  $Y_M$  is influenced mainly by the elastic contribution where the inelastic contributions are smaller. The amplitudes  $Y_E$  and  $Y_3$  are more constrained than  $Y_M$  as suggested by the computed error bands. For  $Y_E$ , and at large  $Q^2$  values, my results are closer to calculations assuming inelastic contributions, elastic +  $\Delta(1232)$  resonance and to a lesser extent elastic +  $\pi N$ , suggesting that  $Y_E$  is influenced mainly by inelastic contributions at large  $Q^2$  values. For  $Y_3$ , the amplitude is flat and above calculations up to  $Q^2 \sim 1.0$  (GeV/c) $^2$  where it starts to fall-off rapidly with increasing  $Q^2$  disagreeing noticeably with theoretical predictions except for calculations assuming elastic

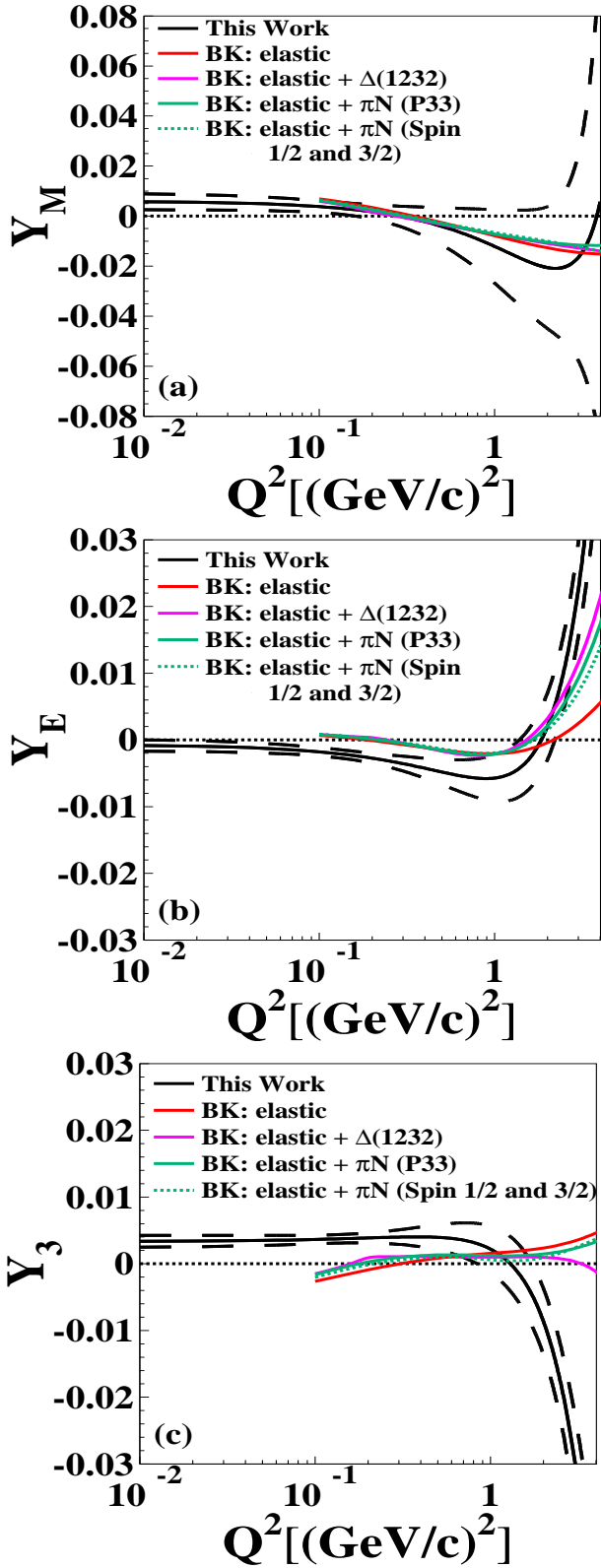


FIG. 6: (Color online) The extracted TPE amplitudes from this work:  $Y_M$  (top),  $Y_E$  (middle), and  $Y_3$  (bottom) as a function of  $Q^2$  at fixed  $\varepsilon = 0.25$  (solid black lines). The error bands on the amplitudes are shown as very long-dashed black lines. In addition, I compare the results to several previous hadronic TPE calculations assuming different intermediate states: elastic “BK: elastic” [28] (solid red line), elastic +  $\Delta(1232)$  “BK:  $\Delta(1232)$ ” [30] (solid magenta line), elastic +  $\pi N$  ( $P_{33}$ ) channel “BK: elastic +  $\pi N$  ( $P_{33}$ )” [31] (solid dark-green line), and elastic +  $\pi N$  (Spin 1/2 and 3/2 Channels) “BK: elastic +  $\pi N$  (Spin 1/2 and 3/2)” [32] (dashed dark-green line).

+  $\Delta(1232)$  resonance which predict a slower fall-off of the amplitude at large  $Q^2$  values. The tension between the  $Y_E$  and  $Y_3$  amplitudes is obvious where they tend partially to cancel each other indicating that the TPE correction to  $\sigma_R$  is driven mainly by  $Y_M$  and to a lesser extent by  $Y_3$ .

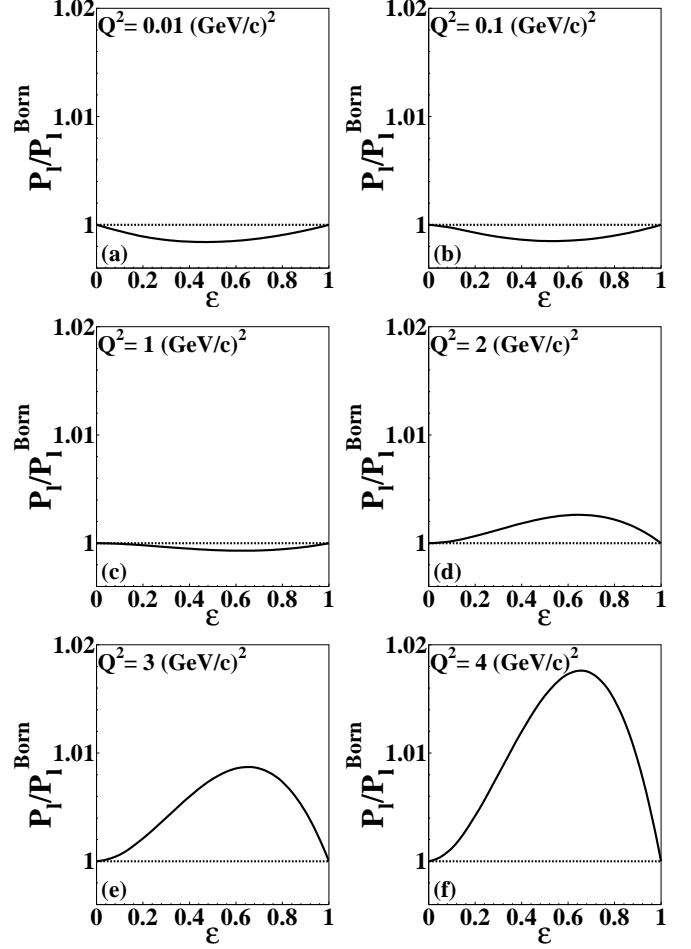


FIG. 7: (Color online) The ratio  $P_l/P_l^{\text{Born}}$  as a function of  $\varepsilon$  as determined using my parametrizations of the TPE amplitudes and Eq. (9c) at the  $Q^2$  value listed in the figure (solid black line).

The  $\varepsilon$  dependence of the ratio  $P_l/P_l^{\text{Born}}$  as extracted from this work, using Eq. (9c), is shown in Fig. 7 for a range of  $Q^2$  values. At low  $Q^2$ , the ratio is below unity and shows little sensitivity to  $\varepsilon$ . The ratio increases with increasing  $Q^2$  and changes sign, where it shows a sign of enhancement with  $\varepsilon$  at large  $Q^2$  values. Figure 8 shows the  $\varepsilon$  dependence of the ratio  $P_l/P_l^{\text{Born}}$  as extracted from this work at  $Q^2 = 2.50$  ( $\text{GeV}/c$ )<sup>2</sup>. I also compare the results to the experimental data points from the GEp-2 $\gamma$  collaboration [56], previous fits from Ref. [46], labelled as “Guttman Fit I” and “Guttman Fit II”, as well as to several theoretical predictions: hadronic TPE calculation from Ref. [13] “Hadronic” where all the proton interme-

diate states are accounted for, the partonic model from Ref. [23] which accounts for hard scattering of electrons by quarks embedded in the nucleon through generalized parton distributions “GPD”, calculation based on QCD factorization within the SCET approach from Ref. [18] arising from both the soft-spectator “KV-Soft Spectator” and hard-spectator “KV-Hard Spectator” scattering contributions, and calculation based on subtracted dispersion relation formalism applied to the case of a nucleon in the intermediate state from Ref. [19] “MV”. While my results show enhancement with  $\varepsilon$ , and are in good qualitative agreement with the experimental data and previous fits at low  $\varepsilon$ , they disagree strongly at large  $\varepsilon$ . On the other hand, my results disagree noticeably with theoretical predictions for the entire  $\varepsilon$  range. The non-vanishing of the ratio  $P_l/P_l^{\text{Born}}$  and the TPE amplitudes  $Y_{(M,3)}$  at  $\varepsilon = 1$  is clearly a behaviour that is mainly associated with the soft-spectator contribution.

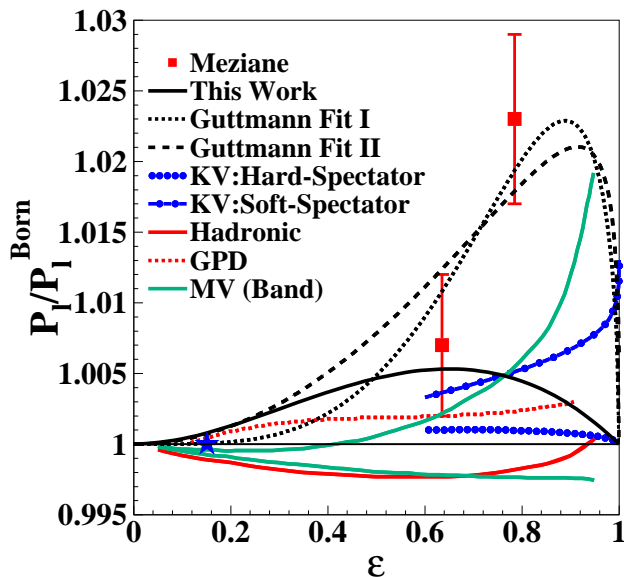


FIG. 8: (Color online) The extracted ratio  $P_l/P_l^{\text{Born}}$  as a function of  $\varepsilon$  at  $Q^2 = 2.50$  ( $\text{GeV}/c$ )<sup>2</sup> from this work (solid black line). Also shown the data points from the GEp-2 $\gamma$  experiment Ref. [56] (solid red squares). The blue star indicates the value of  $\varepsilon$  at which the data have been normalized to unity. In addition, I compare the results to previous fits from Ref. [46] “Guttman Fit I” (dashed black line) and “Guttman Fit II” (long-dashed black line), and to several previous theoretical predictions: “Hadronic” [13] (solid red line), “GPD” [23] (dashed red line), “KV-Soft Spectator” (solid blue line) and “KV-hard Spectator” (dashed blue line) [18], and “MV” [19] prediction band (solid dark-green lines).

## V. CONCLUSIONS

In conclusion, I improved on and extended to low- and high- $Q^2$  values the previous phenomenological ex-

tractions [46] of the three TPE amplitudes and the ratio  $P_l/P_l^{\text{Born}}$  based on the formalism of Guichon and Vanderhaeghen [9]. Assuming that the TPE correction is responsible mainly for the discrepancy between the cross section and polarization data measurements, and because the recoil polarization data were confirmed “*experimentally*” to be essentially independent of  $\varepsilon$  [56], I constrained the ratio  $-\sqrt{\tau(1+\varepsilon)}/(2\varepsilon)P_t/P_l$  in Eq. (9b) to its  $\varepsilon$ -independent term (Born value) by setting the TPE contributions to zero. That allowed for  $\sigma_R/(G_M^p)^2$ , Eq. (9a), to be expressed in terms of the remaining  $Y_E(\varepsilon, Q^2)$  and  $Y_3(\varepsilon, Q^2)$  amplitudes. As these amplitudes are functions of  $\varepsilon$  and  $Q^2$ , I expand each of the amplitudes  $Y_E$  and  $Y_3$  as a second-order polynomial to reserve as possible the linearity of  $\sigma_R$  as well as to account for possible nonlinearities in the TPE amplitudes. Further, I imposed the Regge limit where the TPE correction to  $\sigma_R$  and the TPE amplitudes vanishes in the limit  $\varepsilon \rightarrow 1$  allowing for  $\sigma_R/(G_M^p)^2$  to be expressed in its final form as given by Eq. (15). By fixing  $(G_M^p)^2$  and the recoil polarization ratio  $R$  in Eq. (15), I fit the world data on  $\sigma_R$  used in the analysis of Ref. [52] and extract the TPE amplitudes coefficients  $\alpha_{(0,1,2)}(Q^2)$  and  $\beta_{(0,1,2)}(Q^2)$  which were then used to construct the three TPE amplitudes and the ratio  $P_l/P_l^{\text{Born}}$ . My  $\sigma_R$  fits described the data remarkably well with some deviation from linearity observed at low  $\varepsilon$  for the high  $Q^2$  points in agreement with several hadronic- and pQCD-based calculations in this range.

For  $(G_E^p/G_D(Q^2))^2$ , my results in general are in reasonably good agreement with extractions using calculated TPE corrections and phenomenological-based fits. For  $(G_M^p/\mu_p G_D(Q^2))^2$  and at low  $Q^2$ , my results are significantly above most previous fits. This reflects the discrepancy between the recent Mainz data which yields values of  $G_M^p$  which are systematically 2–5% larger than previous world data [66].

The extracted TPE amplitudes coefficients,  $\alpha_k$  and  $\beta_k$  ( $k = 0, 1, 2$ ), are at the few-percentage-points level, and all show hints of oscillatory behaviour below  $Q^2 = 1.0$  ( $\text{GeV}/c$ )<sup>2</sup> with clear sign of structure (dips/bumps) at  $Q^2 \approx 0.02$  ( $\text{GeV}/c$ )<sup>2</sup>. For  $Q^2 \gtrsim 1.0$  ( $\text{GeV}/c$ )<sup>2</sup>, the coefficients changed sign and increased in magnitude with increasing  $Q^2$ . They were all best parametrized using second-order polynomials. See Table I.

The extracted TPE amplitudes from this work are on the few-percentage-points level, and behave roughly linearly with  $\varepsilon$  as  $Q^2$  increases where they become nonlinear at high  $Q^2$  values. The amplitudes  $Y_M$  and  $Y_3$  are mainly positive at low  $Q^2$  and change sign and grow in magnitude with increasing  $Q^2$ . On the other hand, the amplitude  $Y_E$  is negligible and mainly negative at low  $Q^2$  and changes sign and grows in magnitude with increasing  $Q^2$ . While the  $Y_E$  and  $Y_3$  amplitudes differ in magnitude, they certainly have opposite sign to each other as  $Q^2$  increases where they tend to partially cancel each other. This suggests that the TPE correction to  $\sigma_R$  is driven mainly by  $Y_M$  and to a lesser extent by  $Y_3$  in agreement with previous phenomenological extractions [46] at  $Q^2 =$

2.50 (GeV/c)<sup>2</sup>. My extractions for  $Y_M$  and  $Y_E$  are also in reasonable qualitative agreement with previous hadronic calculations [28, 30–32], all showing the fall and rise of both amplitudes with increasing  $Q^2$ . However, my  $Y_3$  has opposite sign and deviates strongly from both previous extractions and theoretical predictions except at  $Q^2 \sim 1.0$  (GeV/c)<sup>2</sup>.

I also investigated the  $Q^2$  dependence of the TPE amplitudes at a fixed  $\varepsilon = 0.25$ . Both  $Y_M$  and  $Y_E$  fall below theoretical predictions, but they generally are in reasonable qualitative agreement with hadronic theoretical predictions, all showing a fall and then rise of both amplitudes with increasing  $Q^2$ . At large  $Q^2$ , and while my results for  $Y_M$  are closer to calculations assuming a pure proton in the intermediate state (elastic) suggesting that  $Y_M$  is influenced mainly by elastic contributions, my results for  $Y_E$  are closer to calculations assuming inelastic contributions, mainly elastic +  $\Delta(1232)$  resonance and to a lesser extent elastic +  $\pi N$ , suggesting that  $Y_E$  is driven mainly by these contributions. For  $Y_3$  and at low  $Q^2$ , the amplitude is flat and above calculations up to  $Q^2 \sim 1.0$  (GeV/c)<sup>2</sup>. At high  $Q^2$ ,  $Y_3$  starts to fall-off rapidly with increasing  $Q^2$  agreeing only with calculations assuming elastic +  $\Delta(1232)$  resonance which predict a slower fall-off at large  $Q^2$ . I also see clear tension between the  $Y_E$

and  $Y_3$  amplitudes where they tend partially to cancel each other suggesting that the TPE correction to  $\sigma_R$  is driven mainly by  $Y_M$  and to a lesser extent by  $Y_3$ .

The  $\varepsilon$  dependence of the ratio  $P_l/P_l^{\text{Born}}$  as extracted from this work suggests that the ratio is below unity with little sensitivity to  $\varepsilon$  at low  $Q^2$  values. With increasing  $Q^2$ , the ratio increases and changes sign with a sign of enhancement with  $\varepsilon$ . The results at  $Q^2 = 2.50$  (GeV/c)<sup>2</sup> show clear enhancement with  $\varepsilon$ , and are in good qualitative agreement with the experimental data from the GEp-2 $\gamma$  collaboration [56] and previous fits of Ref. [46] at low  $\varepsilon$ , but they disagree noticeably at large  $\varepsilon$ . On the other hand, my results disagree strongly with theoretical predictions for the entire  $\varepsilon$  range.

### Acknowledgments

This work was supported by Khalifa University of Science and Technology. I am grateful to Dr. Dmitry Borisjuk for providing me with his hadronic TPE calculations. I also thank Dr. D. Homouz for his technical assistance, and Dr. S. Phoenix for reading the manuscript and making valuable comments and suggestions.

- 
- [1] R. G. Sachs, Phys. Rev. **126**, 2256 (1962).
  - [2] M. N. Rosenbluth, Phys. Rev. **79**, 615 (1950).
  - [3] N. Dombey, Rev. Mod. Phys. **41**, 236 (1969).
  - [4] A. I. Akhiezer and M. P. Rekalo, Sov. J. Part. Nucl. **4**, 277 (1974).
  - [5] R. G. Arnold, C. E. Carlson, and F. Gross, Phys. Rev. **C23**, 363 (1981).
  - [6] I. A. Qattan *et al.*, Phys. Rev. Lett. **94**, 142301 (2005).
  - [7] J. Arrington, C. Roberts, and J. Zanotti, J. Phys. **G34**, S23 (2007).
  - [8] C. Perdrisat, V. Punjabi, and M. Vanderhaeghen, Prog. Part. Nucl. Phys. **59**, 694 (2007).
  - [9] P. A. M. Guichon and M. Vanderhaeghen, Phys. Rev. Lett. **91**, 142303 (2003).
  - [10] J. Arrington, Phys. Rev. **C68**, 034325 (2003).
  - [11] J. Arrington, Phys. Rev. **C69**, 022201 (R) (2004).
  - [12] P. G. Blunden, W. Melnitchouk, and J. A. Tjon, Phys. Rev. Lett. **91**, 142304 (2003).
  - [13] P. G. Blunden, W. Melnitchouk, and J. A. Tjon, Phys. Rev. **C72**, 034612 (2005).
  - [14] S. Kondratyuk, P. G. Blunden, W. Melnitchouk, and J. A. Tjon, Phys. Rev. Lett. **95**, 172503 (2005).
  - [15] S. Kondratyuk and P. G. Blunden, Phys. Rev. **C75**, 038201 (2007).
  - [16] N. Kivel and M. Vanderhaeghen, Phys. Rev. Lett. **103**, 092004 (2009).
  - [17] N. Kivel and M. Vanderhaeghen, Phys. Rev. **D83**, 093005 (2011).
  - [18] N. Kivel and M. Vanderhaeghen, J. High Energy Physics **1304**, 29 (2013).
  - [19] O. Tomalak and M. Vanderhaeghen, Eur. Phys. J. **A51**, 24 (2015).
  - [20] O. Tomalak and M. Vanderhaeghen, (2015), arXiv:1508.03759 [hep-ph].
  - [21] I. T. Lorenz, Ulf-G. Meißner, H.-W. Hammer, and Y.-B. Dong, Phys. Rev. **D91**, 014023 (2015).
  - [22] Y. C. Chen, A. Afanasev, S. J. Brodsky, C. E. Carlson, and M. Vanderhaeghen, Phys. Rev. Lett. **93**, 122301 (2004).
  - [23] A. Afanasev, S. J. Brodsky, C. E. Carlson, Y. C. Chen, and M. Vanderhaeghen, Phys. Rev. **D93**, 013008 (2005).
  - [24] Y. M. Bystritskiy, E. A. Kuraev, and E. Tomasi-Gustafsson, Phys. Rev. **C75**, 015207 (2007).
  - [25] E. Tomasi-Gustafsson and G. I. Gakh, Phys. Rev. C **72**, 015209 (2005).
  - [26] D. Borisjuk and A. Kobushkin, Phys. Rev. **C74**, 065203 (2006).
  - [27] D. Borisjuk and A. Kobushkin, Phys. Rev. **C75**, 038202 (2007).
  - [28] D. Borisjuk and A. Kobushkin, Phys. Rev. **C78**, 025208 (2008).
  - [29] D. Borisjuk and A. Kobushkin, Phys. Rev. **D79**, 034001 (2009).
  - [30] D. Borisjuk and A. Kobushkin, Phys. Rev. **C86**, 055204 (2012).
  - [31] D. Borisjuk and A. Kobushkin, Phys. Rev. **C89**, 025204 (2014).
  - [32] D. Borisjuk and A. Kobushkin, Phys. Rev. **C92**, 035204 (2015).
  - [33] Hai Qing Zhou, Chung Wen Kao, and Shin Nan Yang, Phys. Rev. Lett. **99**, 262001 (2007), and [Erratum-ibid. Phys. Rev. Lett. **100**, 059903 (2008)].
  - [34] Hai-Qing Zhou, Chin. Phys. Lett. **26**, 061201 (2009).
  - [35] Hai-Qing Zhou, and Shin Nan Yang, Eur. Phys. J. **A51**,

- 105 (2015).
- [36] Krzysztof M. Graczyk, and Cezary Juszczak, *J. Phys.* **G42**, 034019 (2015).
- [37] Krzysztof M. Graczyk, *Phys. Rev.* **C88**, 065205 (2013).
- [38] Krzysztof M. Graczyk, *Phys. Rev.* **C84**, 034314 (2011).
- [39] V. M. Braun, A. Lenz, and M. Wittmann, *Phys. Rev.* **D73**, 094019 (2006).
- [40] I. A. Qattan, Ph.D. thesis, Northwestern University (2005), arXiv:nucl-ex/0610006.
- [41] V. Tvaskis *et al.*, *Phys. Rev.* **C73**, 025206 (2006).
- [42] D. Borisjuk and A. Kobushkin, *Phys. Rev.* **C76**, 022201(R) (2007).
- [43] D. Borisjuk and A. Kobushkin, *Phys. Rev.* **D83**, 057501 (2011).
- [44] Y.-C. Chen, C.-W. Kao, and S.-N. Yang, *Phys. Lett.* **B652**, 269 (2007).
- [45] J. Arrington, *Phys. Rev.* **C71**, 015202 (2005).
- [46] J. Guttmann, N. Kivel, M. Mezziane, and M. Vanderhaeghen, *Eur. Phys. J.* **A47**, 77 (2011).
- [47] M. P. Rekalo and E. Tomasi-Gustafsson, *Eur. Phys. J.* **A22**, 331 (2004).
- [48] I. A. Qattan and A. Alsaad, *Phys. Rev.* **C83**, 054307 (2011), [Erratum-ibid. **C84**, 029905 (2011)].
- [49] I. A. Qattan, A. Alsaad, and J. Arrington, *Phys. Rev.* **C84**, 054317 (2011).
- [50] I. A. Qattan, and J. Arrington, *Phys. Rev.* **C86**, 065210 (2012).
- [51] I. A. Qattan, and J. Arrington, *Eur. Phys. J. WOC* **66**, 06020 (2014).
- [52] I. A. Qattan, J. Arrington, and A. Alsaad, *Phys. Rev.* **C91**, 065203 (2015).
- [53] J. Arrington, P. Blunden, and W. Melnitchouk, *Prog.Part.Nucl.Phys.* **66**, 782 (2011).
- [54] C. E. Carlson and M. Vanderhaeghen, *Ann. Rev. Nucl. Part. Sci.* **57**, 171 (2007).
- [55] M. E. Christy *et al.*, *Phys. Rev.* **C70**, 015206 (2004).
- [56] M. Mezziane *et al.*, *Phys. Rev. Lett.* **106**, 132501 (2011).
- [57] J. Arrington, *Phys. Rev.* **C69**, 032201 (R) (2004).
- [58] D. Adikaram *et al.* (CLAS Collaboration), *Phys. Rev. Lett.* **114**, 062003 (2015).
- [59] I. A. Rachek *et al.*, *Phys. Rev. Lett.* **114**, 062005 (2015).
- [60] L. Andivahis *et al.*, *Phys. Rev.* **D50**, 5491 (1994).
- [61] R. C. Walker *et al.*, *Phys. Rev.* **D49**, 5671 (1994).
- [62] See Supplemental Material at [to be inserted] for the proton form factors, and the TPE amplitudes coefficients from this work.
- [63] J. Arrington, W. Melnitchouk, and J. A. Tjon, *Phys. Rev.* **C76**, 035205 (2007).
- [64] S. Venkat, J. Arrington, G. A. Miller, and X. Zhan, *Phys. Rev.* **C83**, 015203 (2011).
- [65] W. Alberico, S. M. Bilenky, C. Giunti, and K. M. Graczyk, *Phys. Rev.* **C79**, 065204 (2009).
- [66] J. C. Bernauer *et al.* (A1 Collaboration), *Phys. Rev.* **C90**, 015206 (2014).
- [67] A. J. R. Puckett *et al.*, *Phys. Rev.* **C85**, 045203 (2012).
- [68] T. Janssens, R. Hofstadter, E. B. Hughes, and M. R. Yearian, *Phys. Rev.* **142**, 922 (1966).